Earth and Planetary Science Letters 536 (2020) 116145

Contents lists available at ScienceDirect

Earth and Planetary Science Letters

www.elsevier.com/locate/epsl

The dynamics of a long-lasting effusive eruption modulated by Earth tides

Stéphanie Dumont [a,b,*], Jean-Louis Le Mouël [c], Vincent Courtillot [c], Fernando Lopes [c], Freysteinn Sigmundsson [d], Diego Coppola [e,f], Eva P.S. Eibl [g], Christopher J. Bean [h]

[a] University of Beira Interior, Covilhã, Portugal
[b] Instituto Dom Luiz (IDL), Faculdade de Ciências, Universidade de Lisboa, Lisboa, Portugal
[c] Institut de Physique du Globe de Paris, Paris, France
[d] Institute of Earth Sciences, University of Iceland, Reykjavik, Iceland
[e] Dipartimento di Scienze della Terra, Universita di Torino, Italy
[f] NatRisk, Centro Interdipartimentale sui Rischi Naturali in Ambiente Montano e Collinare, Università degli Studi di Torino, Italy
[g] University of Potsdam, Potsdam, Germany
[h] Geophysics Section, Dublin Institute for Advanced Studies, Dublin, Ireland

ARTICLE INFO

Article history:
Received 13 November 2019
Received in revised form 30 January 2020
Accepted 7 February 2020
Available online 13 February 2020
Editor: M. Ishii

Keywords:
Holuhraun
Earth tides
effusive eruption
seismic tremor
lava flows
thermal anomalies

ABSTRACT

Deciphering eruptive dynamics in near-real time is essential when dealing with hazard assessment and population evacuation. Recognition of specific patterns in time-series measured during volcanic activity may help decipher distinctive behavior at active volcanoes, providing insights into the underlying driving mechanisms. Multi-parameter data sets usually agree on the overall trend characterizing the temporal evolution of an eruption providing insights into the first-order eruptive dynamics. However, second-order variations detected in different data sets remain often poorly understood. The 2014-2015 Holuhraun eruption (Iceland) offers an excellent opportunity to investigate the dynamics of a long-lasting effusive eruption. We analyze the seismic tremor and the volcanic radiated power emitted by the lava field during the 6 months of the eruption using Singular Spectrum Analysis (SSA). In both geophysical time-series, we identify periods from ~5 to ~32 days coinciding with periods of Earth tides. Here we show that ~50% of both signals are composed of tidal periods suggesting that magma movements follow frequencies imposed by lunisolar forces within the crust and at Earth's surface.

1. Introduction

Periodic and quasi-periodic behaviors at some volcanoes have been detected during eruptive or unrest periods, using geochemical or geophysical measurements and suggesting a certain sensitivity of volcanic systems to lunisolar tidal forces, especially when volcanoes are in a critical state (Hamilton (1973); Mauk and Johnston (1973); Martin and Rose (1981); Stothers (1989); Patanè et al. (1994); Emter (1997); Williams-Jones et al. (2001); Custodio et al. (2003); Melnik et al. (2008); Dinger et al. (2018); Girona et al. (2018)). Clear cyclic oscillations with periods ranging from hours to diurnal have been detected: they appear to modulate seismicity during unrest (Mauk and Kienle (1973); Girona et al. (2018); Petrosino et al. (2018); Ricco et al. (2019)) as well as eruptive activity through the frequency/intensity of explosive phases or continuous degassing (Williams-Jones et al. (2001); Sottili et al. (2007); Cigolini et al. (2009); Sottili and Palladino (2012); Bredemeyer and Hansteen (2014); Dinger et al. (2018)). Tidal forces have also been suggested to increase the likelihood of eruption onset for instance at Kilauea (Hawaii), Fuego (Guatemala) and Mayon (Philippines) (Mauk and Johnston (1973); Dzurisin (1980); Martin and Rose (1981); Jentzsch et al. (2001)). These studies have revealed a specific response of volcanic systems to the fortnightly, diurnal and semi-diurnal tides. However, tidal stresses are of small amplitude, a few 10^3 Pa for the fortnightly, compared to tectonic stresses on the order of 10^6-10^8 Pa (Sparks, 1981). Recognition of tidal periods in time-series measurements at volcanoes has not been systematic, suggesting that all volcanoes do not seem to respond in the same way to the Moon-Sun gravitational forces (Sparks (1981); Emter (1997); Neuberg (2000); van Manen et al. (2010)). These interactions and their mechanisms are therefore still a debated topic.

Using data from the 2014-2015 Holuhraun eruption (Iceland), we investigate the dynamics of a long-lasting effusive eruption with a focus on processes interfering with the driving pressure

* Corresponding author at: University of Beira Interior, Covilhã, Portugal.
E-mail address: sdumont@segal.ubi.pt (S. Dumont).

https://doi.org/10.1016/j.epsl.2020.116145
0012-821X/

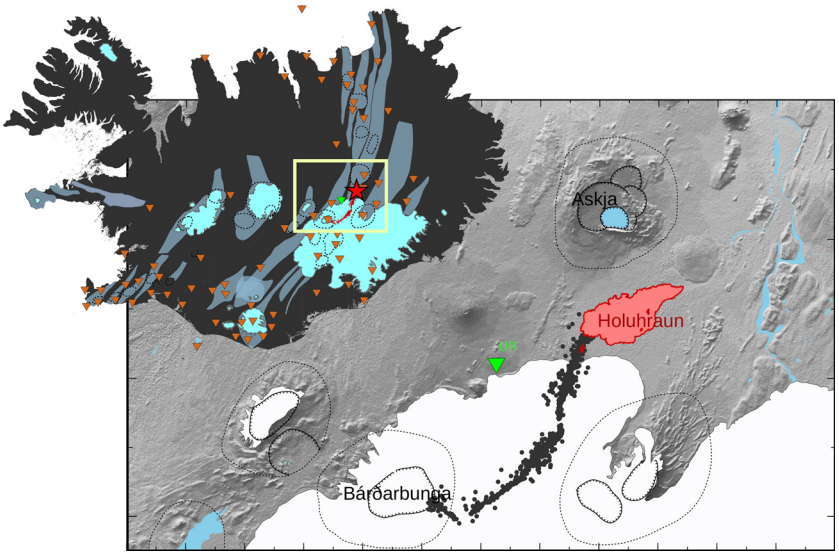

Fig. 1. The 2014-2015 volcano-tectonic activity beneath Vanatjökull glacier (Iceland) and the seismic network. Inset showing the volcano-tectonic map of Iceland with the central volcanoes (dashed lines) and the associated fissure swarms (gray areas) that form the neovolcanic zones (Johannesson and Saemundsson (2009)) and also the glaciers (cyan). The red dots show the seismicity prior to the onset of the eruption, from 16 August to 6 September 2014 (Sigmundsson et al. (2015)), similarly to the black dots in the main figure. The eruption site is indicated by the red star. The instruments used to quantify the seismic tremor include SIL seismic network (inverted brown triangles), a seismic array deployed by UCD within the FutureVolc project framework (inverted green triangles, Eibl et al. (2017a,b)). For more details on the configuration on the 7-station array, see Eibl et al. (2017b). Holuhraun lava field is shown with red surface. (For interpretation of the colors in the figure(s), the reader is referred to the web version of this article.)

source and on how external processes may affect the course of an eruption. This effusive eruption initiated after the propagation of a 48-km long dyke at the Icelandic divergent plate boundary and produced a lava field whose bulk volume of 1.4 ± 0.2 km^3 (Fig. 1), making it the largest eruption in Iceland since the 1783-1784 Laki eruption (Gudmundsson et al. (2016); Pedersen et al. (2017)). Activity was closely monitored by multi-parameter sensors before, during and after the eruption, despite the challenging conditions in one of the most remote places in Iceland (Fig. 1; Sigmundsson et al. (2015); Ágústsdóttir et al. (2016); Gudmundsson et al. (2016); Coppola et al. (2017); Eibl et al. (2017a); Parks et al. (2017); Pfeffer et al. (2018); Dumont et al. (2018)). In this paper, we study variations in the seismic tremor that provide insights into magma flow from depth to surface and in the power radiated by the lava field that reflects the eruptive dynamics at the surface through the growth of the lava field. Both seismic tremor (ST) and volcanic radiated power (VRP) data were analyzed for the whole eruption period using the technique of Singular Spectrum analysis (SSA). Contrary to other spectrum analysis methods, SSA provides information on the temporal evolution (phase shift, attenuation) of the components forming the geophysical signals and their contribution to the original time-series. We compare the SSA spectral components of ST and VRP with those of the length-of-day (l.o.d.), a relevant measure of the tidal actions on the Earth's rotation velocity (Lambeck (2005); Ray and Erofeeva (2014); Lopes et al. (2017); Le Mouël et al. (2019)) whose variations have also been evoked to affect volcanism (Palladino and Sottili (2014); Sottili et al. (2015); Lambert and Sottili (2019)). Long-term periods including decadal variations in the l.o.d. have been attributed to core/mantle interactions while shorter periods are caused by external modulation and in particular by tidal forces (Jault and Le Mouël (1991); Lambeck (2005)). The redistribution of the solid earth and ocean masses induced by lunisolar gravitational forces affects also the atmosphere. These three layers being coupled, their modulation by tidal forces influences as well their interaction (Lambeck (2005)). Although the solid tides are the most important, all three periodic tidal deformations lead to perturbations of the inertia tensor, thus directly impacting the polar motion and therefore the Earth's rotation velocity and of course the l.o.d. (Lambeck (2005)). In past studies, the influence of earth tides on volcanism has been suggested using theoretical estimates of the tidal potential (see (Neuberg, 2000; Petrosino et al., 2018) for instance). With our approach, we preferred using observations instead of models. Data include by essence the space-time evolution of the complex interaction of the Earth, Moon and Sun, whose calculations become much more complicated if the complexity of the trajectories of the three celestial bodies and their variations are taken into account. This way, the comparison of observations of seismic tremor, volcanic radiated power and length-of-day allows us to shed light on the influence of Earth tides on magma movements from the plumbing system to the surface, over the course of the 6-month long lava flow emplacement at Holuhraun.

2. Data and methods

2.1. Seismic tremor

We consider the temporal evolution of the 2014-2015 volcanic activity at Holuhraun through the seismic tremor and the energy radiated by the lava field over the 6 months of the eruption. The seismic tremor was recorded during Holuhraun eruption by the national seismic network (SIL) and a 7-station array located 12 km from the eruptive fissure (Fig. 1; Eibl et al. (2017b)). The data were collected every 0.01 s. The amplitude of the seismic signal was initially instrument-corrected, detrended, tapered and filtered between 0.8 and 2.0 Hz and its root median square was calculated to represent the tremor amplitude as described by Eibl et al. (2017a,b).

2.2. Volcanic radiated power

Thermal anomalies at Earth's surface can be detected by the Moderate Resolution Imaging Spectroradiometer onboard satellite sensor (MODIS). At latitudes of Iceland, Terra and Aqua satellites have between 6 and 10 acquisitions per day due to their polar, sun-synchronous orbit (Coppola et al. (2019)). The MIROVA system for Middle InfraRed Observation of Volcanic Activity, was

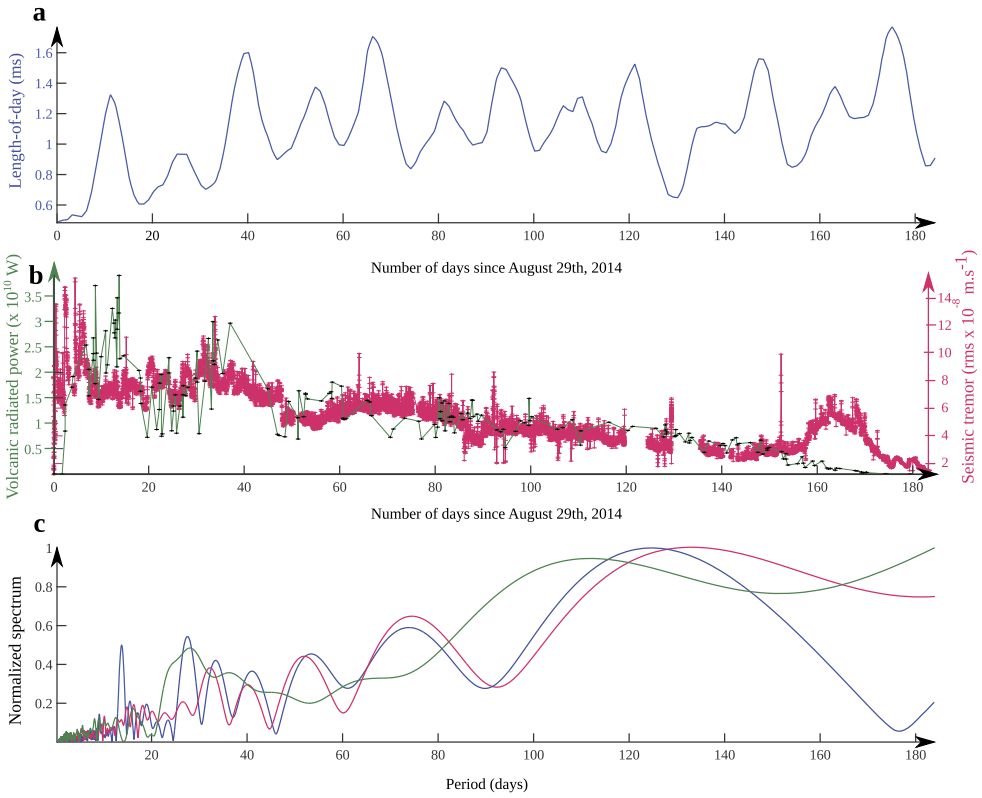

Fig. 2. Seismic tremor and volcanic radiated power time-series associated with the 2014-2015 Holuhraun eruption. Time-series for the length-of-day (a), seismic tremor and radiated power emitted by the lava field (b) during Holuhraun eruption from 29 August 2014 to 27 February 2015. Original data published in Coppola et al. (2017, 2019) and Eibl et al. (2017a)). The corresponding spectra are presented in the last figure (c) using the same color code.

developed in the last decade to enhance volcanic hot-spot detection and track their evolution using near real-time processing of MODIS data (Coppola et al. (2016)). MIROVA relies on an algorithm that combines both spectral and spatial approaches and automatically detects and locates high-temperature thermal anomalies using middle (MIR) and thermal (TIR) infrared bands resulting in the quantification of the volcanic radiant power (VRP). For more details, see Coppola et al. (2016, 2019).

2.3. Length-of-day

It has been known for decades that the Earth's rotation velocity whose measure is the length-of-day (l.o.d.), shows variations at different time scales (Guinot (1973)). The slow overall deceleration observed corresponds to a sum of pseudo-periodic and oscillating trends caused by the astronomical forces that slow down Earth's rotation. The decelerating rate is of the order of 2 ms per century and takes its origin in lunar forces. The l.o.d. is an astronomical measure, estimated daily by a combination of laser and satellite (VLBI) measurements. For more details, see Jault and Le Mouël (1991) and Lambeck (2005). For this study, we will use the data set EOP14C04 (https://www.iers.org/IERS/EN/DataProducts/EarthOrientationData/eop.html), provided by the International Earth Rotation Service (IERS, Paris, France).

2.4. Singular spectrum analysis

Singular Spectrum Analysis (SSA) is a general formulation of the spectral decomposition formulated by Vautard and Ghil (1989) and Vautard et al. (1992). It is a powerful, non-parametric, time series analysis tool based on the Karhunen-Love spectral decomposition (Kittler and Young (1973)). SSA decomposes a time-series into a sum of a small number of independent components that can be identified as either a trend, periodic or quasi-periodic component or noise. The first step of the decomposition consists in building a trajectory or Hankel matrix. The time-series vector of length N, allows to create lagged copies of length L and thus to create the Hankel matrix of size $L \times K$ with $K = N - L + 1$. With the next step, Singular Value Decomposition or SVD (Golub and Kahan (1965)) is applied to the Hankel matrix allowing to identify the eigen values composing the time-series. The resulting eigen values are ranked in decreasing order of magnitude with the first ones representing those with a larger contribution to the original signal. Groups of very similar eigen values are then assembled to form the main components that are used to reconstruct the original signal. For further details on the method and its application, see Lopes et al. (2017) and Le Mouël et al. (2019).

3. Results

3.1. Volcanic time-series and the contribution of Earth tides

The reference date we used in this study is 29 August 2014. It is 13 days after initiation of the dyke propagation from Bárdarbunga caldera, and two days prior to the onset of the six-month eruption, when a 4-hour eruption took place, at the same place as the main eruption that initiated two days later (Sigmundsson et al. (2015); Pedersen et al. (2017)). Seismic tremor reached the largest values with the onset of the main eruption on 31 August 2014, remained high up to 5 September 2014 (Fig. 2b), while the lava fountaining was still intense with the highest fountains recorded on 4 September (Eibl et al., 2017a). It then shows an overall decline over the 6 months of the eruption. The VRP shows a very similar temporal trend except for its maximum (Fig. 2b), that is only reached around 7-11 September 2014. The time difference between maxima in VRP and seismic tremor may actually be induced by the

Table 1
Periods composing the seismic tremor and VRP time-series. Periods of lunisolar tides detected in the l.o.d., seismic tremor and volcanic radiative power were identified after Ray and Erofeeva (2014).

Ray and Erofeeva (2014) (days)	l.o.d. (days)	Seismic tremor (days)	Radiative power (days)	Earth tide names	Origin L: Moon; S: Sun
31.96	33.95 ± 3.62	32.00 ± 2.28		MSm	L + S
25.62	26.66 ± 2.42		24.28 ± 4.99	Mm	L
23.85		23.76 ± 3.08		Mm	L
	16.64 ± 1.32	16.60 ± 1.06	16.01 ± 1.57	MSm[1]	L + S
15.91			15.76 ± 1.24	MSm[1]	L + S
13.66	13.65 ± 0.61	13.52 ± 1.56	13.00 ± 2.69	Mf	L
12.78		12.58 ± 1.59	12.30 ± 2.79	Mf	L
9.13	9.13 ± 0.67	9.33 ± 0.43		Mtm	L
7.23	7.22 ± 0.21	7.28 ± 0.21	7.22 ± 0.32	Mt	L
5.40		5.40 ± 0.27	5.38 ± 0.18	MSp	L + S

[1] Harmonic of MSm.

lava flow thermal regime. Transient phases seem to characterize the thermal regime of lava flows as long as their maximal length has not been reached reflecting conditions to attain a thermal equilibrium (Coppola et al. (2019) and references therein). Field and satellite observations from Pedersen et al. (2017) confirmed that the maximal length of the first and main lava channel was reached between 7-15 September 2014. Eibl et al. (2017a) jointly analyzed both signals without finding any clear correlation except in the first-order decrease that was also observed using other geophysical measurements (Gudmundsson et al. (2016)). For a more detailed description of the temporal evolution of these two parameters and the derived effusion rate, see Coppola et al. (2017, 2019) and Eibl et al. (2017a). During the ∼180 days of eruption, the l.o.d. shows a small overall increase punctuated by (pseudo) periodic oscillations showing larger amplitude variations (Fig. 2a), known as the result of lunisolar forces acting on the Earth's rotation velocity (Le Mouël et al. (2019)). The comparison of the spectra associated with the seismic tremor, VRP and l.o.d. (Fig. 2c), highlights a clear feature: the seismic tremor and l.o.d. have a very similar spectral content for periods longer than 30 days, although the length of the present data set prevents a proper representation and interpretation of periods longer than 45-60 days.

The first 9 and 8 components (corresponding to 17 and 15 eigenvalues, see Section Data and Methods) of the seismic tremor and VRP signals respectively, were considered to analyze the spectral content of the two time-series (Fig. 3a-c). As we show with the reconstructed signals in Fig. 3, these first 9 and 8 components account for most variations of the original time-series. It is striking to note that most of these first components of the seismic tremor and VRP match well-known Earth tides that are observed in the l.o.d. time-series (Fig. 3 and Table 1). Actually, taking into account all lunisolar periods identified in each time-series, reveals that 53.6% of the tremor and 51.6% of the VRP variations correspond to lunisolar tides (Fig. 3 and Table 1). Further results are shown with Fig. 4 sorted according to the decreasing amplitude of the tidal components extracted in the l.o.d. The figure shows both the waveforms of the extracted component and the corresponding spectrum. Relying on the Parseval theorem that states that the information of a signal spectrum is similar to the signal itself, we define the uncertainty of identified periods by the half-width of their peaks at half-height.

Fig. 4a presents the signals and the Fourier spectra associated with the main tide, the fortnightly, characterized by a ∼13.66 days period for the seismic tremor, radiated power and the l.o.d., respectively. This lunar tide is the strongest in amplitude (see Ray and Erofeeva (2014), Table 3 or Le Mouël et al. (2019), Table 1). Note that this period is also very close to the 13.63 days period, an harmonic of the solar synodic rotation period (27.27 days). There are therefore two possible sources for modulation of these tidal forces (Lopes et al. (2017)). If we take into account the uncertainties of the periods identified in the Fourier spectra, seismic tremor, radiated power and l.o.d. start in phase at the eruption onset (Fig. 4a). The corresponding wave shapes for the seismic tremor and radiated power attenuate, in contrast to that of the l.o.d. oscillation. Moreover, the attenuation rate and the phase shift between both signals are not the same. This likely reflects the inherent properties of the media where the tidal wave carried by the magma is propagating from the upper crust to the ground surface.

Fig. 4b shows a tidal component of ∼25-days period. Actually, we detect two periods centered at 23.76 days and 24.28 days for the seismic tremor and VRP respectively (Table 1). Their uncertainties are such they can be identified to two very similar periods of the Moon monthly tide (Ray and Erofeeva (2014)). As previously observed for the ∼13.6-days component, both volcanic signals are starting almost in phase with the l.o.d. if we take into account the uncertainties. Their amplitude is also reduced over time, but is less pronounced than previously observed for the fortnightly period. Interestingly, both the ∼13.6 and ∼25-days components of the VRP components appear to be systematically more attenuated than those of the seismic tremor suggesting that this observation is likely related to the medium propagation. The terrestrial surface representing an interface between atmosphere/lithosphere where lava flows, it is indeed much more dispersive for a propagating wave than the upper crust and could therefore explain these differences.

We illustrate other periods, e.g. ∼16 and ∼9 days, identified in our time-series, in Fig. 4c-d. All their waveforms show different behaviors. In the ∼16 days-period, VRP signal is more similar to the l.o.d. than the seismic tremor (Fig. 4c). Actually, the latter shows an amplification over time that is also detected in the ∼9 days period (Fig. 4d). This ∼9 days period corresponds to the second harmonic of the lunar month period and is only detected in the seismic tremor. These observations (Fig. 4) suggest that 1) these tides are not detected in the same way by the propagating magma and the lava field as illustrated by the ∼9 and ∼16-days periods (Fig. 4 and Table 1) and 2) that the amplitude of the seismic tremor is not further systematically attenuated with time.

3.2. *The tidal potential as external mechanism modulating volcanic activity*

With Fig. 4, we compare the periods extracted from the seismic tremor and the power radiated by the lava field with those already known in l.o.d. Although a certain phase shift is detected in some component between the tremor and the lava field with respect to the l.o.d. (likely caused by the volcanic processes), these common periods highlight one common origin, the tidal forces (Fig. 5a), which act on the three geophysical phenomena, despite their different nature. We estimate the first-order (strongest) tidal force (Jobert and Coulomb (1973)), f_r, (see Supplementary Mate-

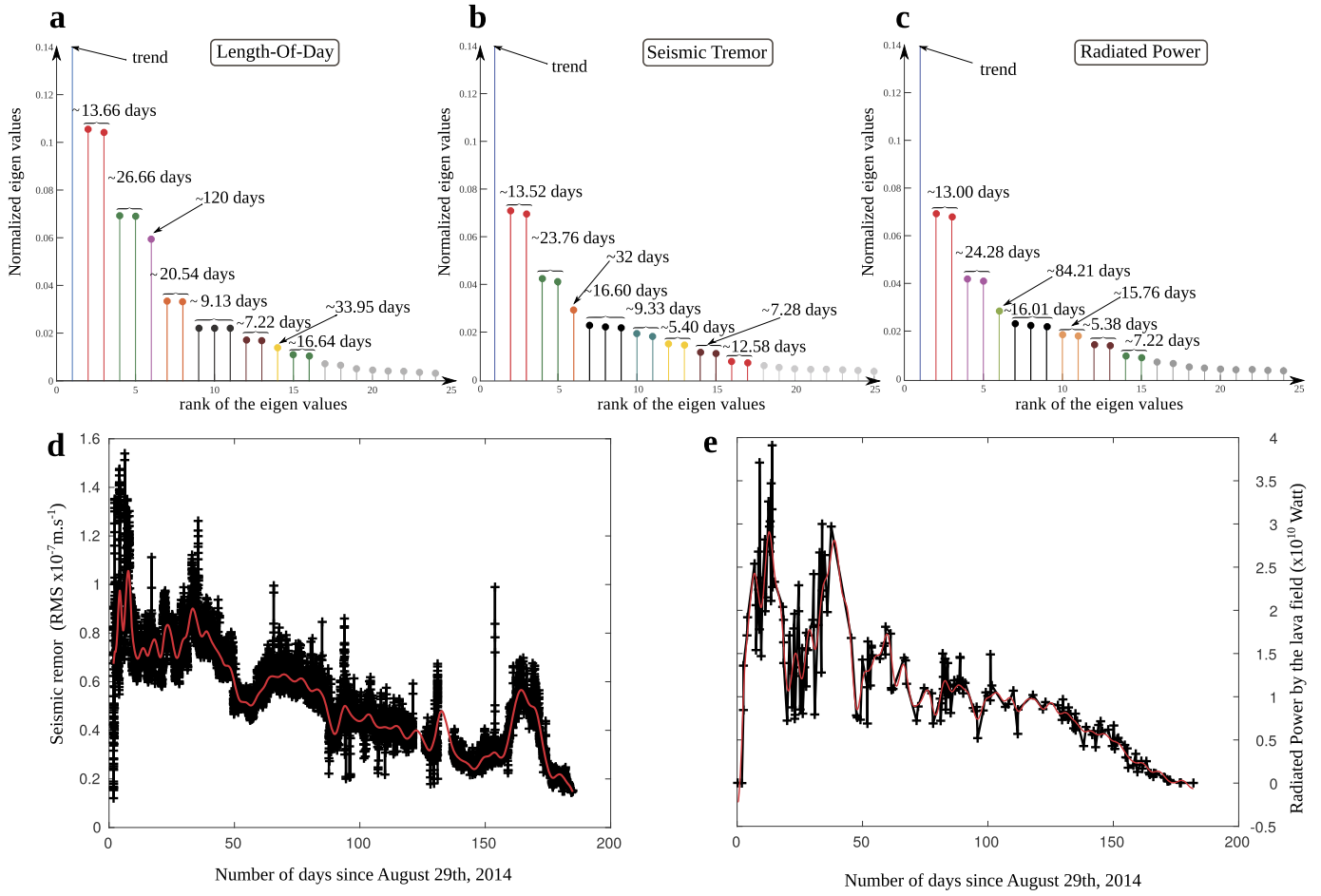

Fig. 3. Decomposition and Reconstruction of the geophysical time-series. Eigen values of the decomposition are ranked in decreasing order of amplitude for the l.o.d. (a), the seismic tremor (b) and the power radiated by the lava field (c). Each color represents components identified using the first 15-17 eigen values and based on the periods recognized in the l.o.d. The trends represent the overall and first-order variation (Supplementary, Figure S1). They are highly dependent on the time interval considered. They are not further discussed in this study despite they represent the highest energy of the time-series. (d-e) Original (black) and reconstructed time-series (red) of the seismic tremor and radiated power by the lava field, respectively. The reconstruction is based on the SSA method using the first 17 and 15 eigen values respectively and allows to explain most the observed variations.

rial and Fig. 5a), that corresponds to the vertical component, acting on a unit mass at the point P on Earth's surface, to be about 5.6 10^{-7} N·kg^{-1}. If we now consider the pressure gradient $\frac{\partial P}{\partial h}$ associated with the tidal action on an area of section S and of thickness dh, we have:

$$\rho f_r S dh = S\frac{\partial P}{\partial h}dh \rightharpoonup \frac{\partial P}{\partial h} = \rho f_r \quad (1)$$

with ρ, the mean density of crust in Icelandic volcanic zones (2400 kg·m^{-3}; Gudmundsson and Högnadóttir (2007)). We integrate the pressure between the surface and 8 km depth corresponding to the upper crust depth range where seismicity was recorded during the dyke propagation preceding the onset of the eruption (Sigmundsson et al. (2015); Woods et al. (2019)). We obtain a pressure of 10.8 Pa, a value that is not sufficient for rock fracturing, the rock strength being at least of 0.1-20 MPa for a basalt in tensile stresses and much higher in compression (Schultz (1996)). However, we suggest this amount is sufficient for Earth tides to drive a fluid flow. Indeed, this force induces a localized stress on the poroelastic medium formed by the subsurface resulting in a spatial pressure gradient that promotes the flow of subsurface fluids (McMillan et al. (2019)). Magma and groundwater at subsurface and Earth's surface may therefore be modulated by such a force as shown by the seismic tremor and VRP.

We further evaluate the timing of the tidal components by calculating the tidal potential for the strongest lunar tide, the fortnightly (13.66-days periods), that also has the strongest energy in all geophysical time-series studied (see Supplementary Material and Figs. 3 and- 5a). We estimate the potential for two sites of observation, one in Iceland ($\theta = 65°$) and one at the Equator ($\theta = 0°$). The result is presented in Fig. 5b. The phase shift detected between the two observation locations (Iceland versus Equator) illustrates the latitude-dependence (zonal distribution) of the fortnightly tide. This phase shift evolves slowly over time such that at the end of the eruption, the zonal tide is almost in phase at the Equator and in Iceland. Moreover, this zonal tide calculated at the Icelandic latitude, appears to be exactly in phase with the fortnightly component identified in the seismic tremor at the start of the eruption (Fig. 5b), and for the following 60 days.

4. Discussion

The Singular Spectrum Analysis applied to the seismic tremor and volcanic radiated power time-series clearly evidence the influence of Sun-Moon gravitational forces on our measurements over the course of Holuhraun eruption. For the first time, we show how 6-8 tidal periods varying from ~5 to ~32 days contribute to two time-series characterizing volcanic processes. Most similar studies on volcanoes have detected the fortnightly, semi-diurnal and diur-

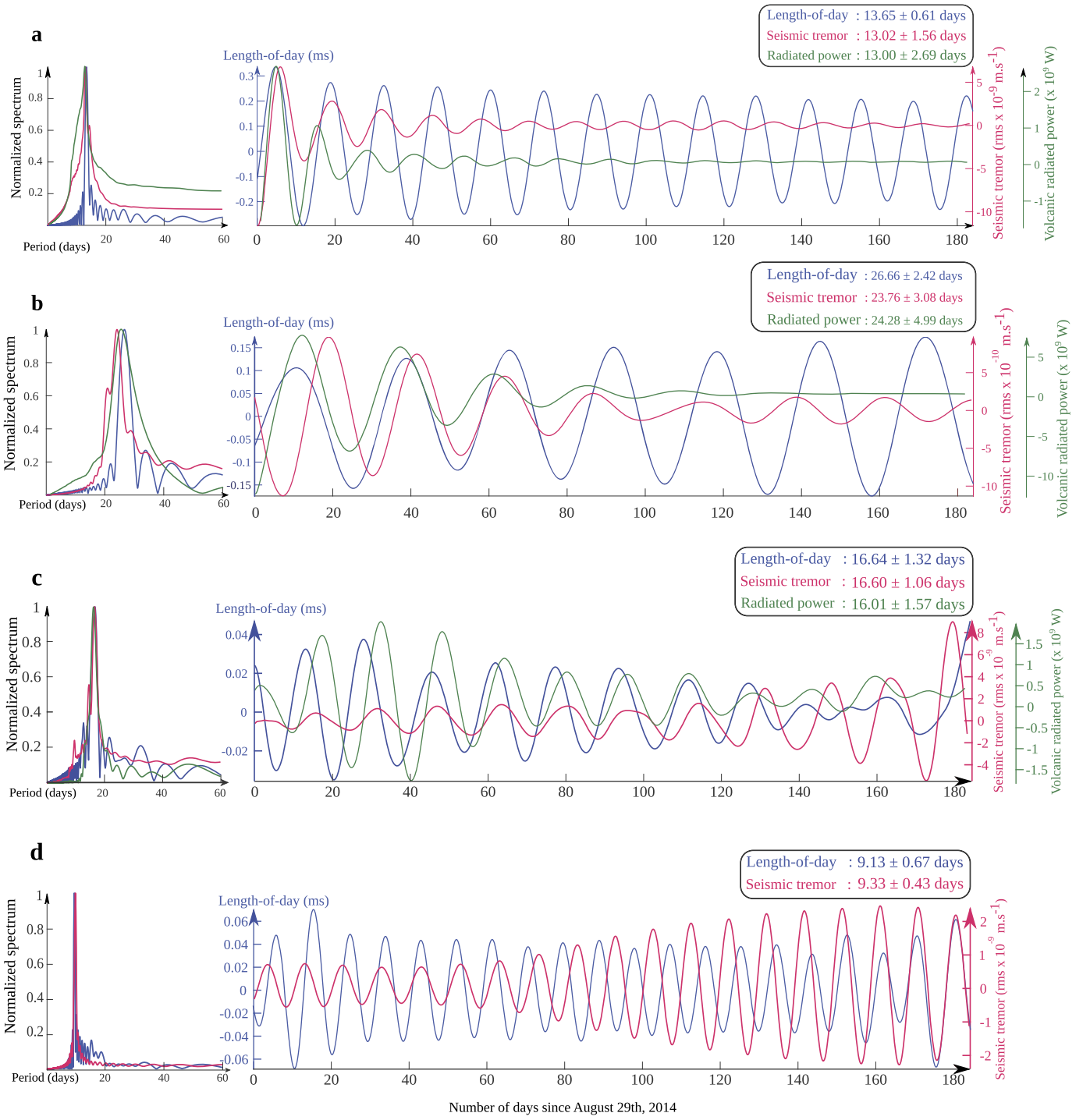

Fig. 4. Components associated with a ∼13, ∼26, ∼16 and ∼9 days periods. (a) Normalized spectrum of the Fourier transform (left) associated with the second SSA component for the l.o.d. (blue), seismic tremor (magenta) and volcanic radiated power emitted by the lava field (green) and the corresponding waveforms (right). A similar representation is adopted for the series of figures in b, c and d. In b, the periodogram and the waveforms represent the third SSA component. This component may correspond to two tides of very similar periods, e.g. ∼26 and ∼24 days, associated with the lunar monthly (Table 1; Ray and Erofeeva (2014)). In c, the ninth SSA component for the l.o.d. is represented along with the fifth component of the seismic tremor and VRP. Finally, in d, the sixth SSA component is plotted for l.o.d. and seismic tremor.

nal tides (Hamilton (1973); Mauk and Johnston (1973); Mauk and Kienle (1973); Dzurisin (1980); Martin and Rose (1981); Stothers (1989); Emter (1997); Williams-Jones et al. (2001); Custodio et al. (2003); Sottili et al. (2007); Dinger et al. (2018); Girona et al. (2018); Ricco et al. (2019)). Only a few studies have detected other tidal periods as for instance, the lunar monthly and the ∼7-day period tides at Stromboli volcano (Sottili and Palladino (2012)) and the periods of 28-33 and 6-9 days at Villarrica and Llaima volcanoes (Bredemeyer and Hansteen (2014)). The techniques adopted to evaluate the correlation between earth tides and physical parameters associated with volcanic processes as well as some data processing applied to the time-series may reduce the detection range of tidal periods (Neuberg (2000)). The temporal resolution of the analyzed time-series may as well directly influence the detection of the different tides and their resolution (van Manen et al. (2010)). Similarly, with this study, we show that the predominant

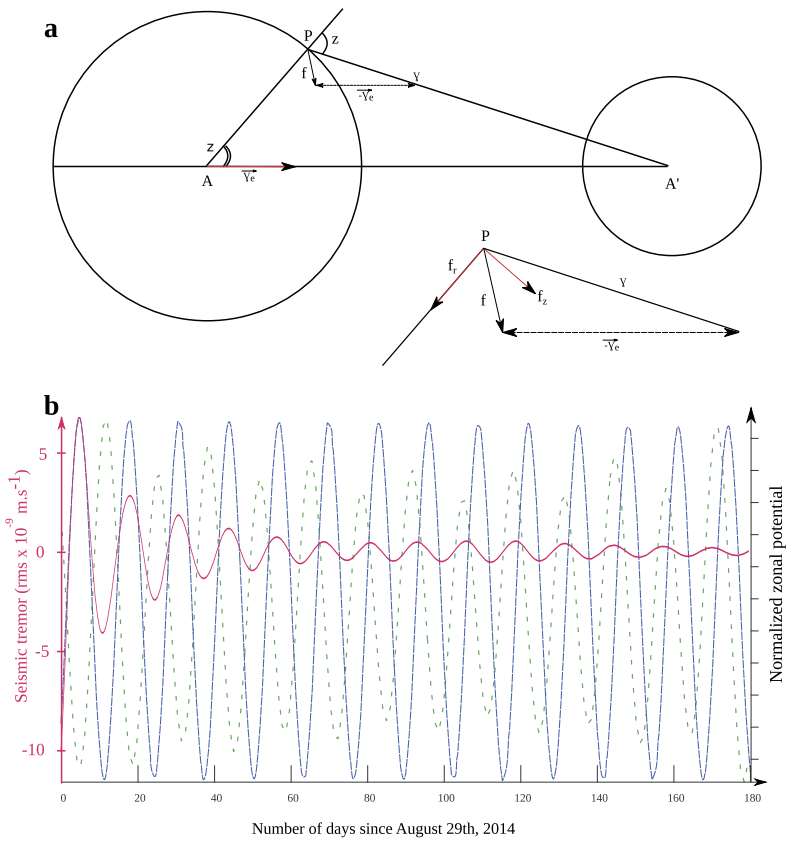

Fig. 5. Tidal force and potential during the eruption. (a) Attraction of (A') body acting on P located at the surface of (A) and the associated tidal force, f as described by Jobert and Coulomb (1973). See Supplementary Material for more details. (b) Zonal tides calculated for the lunar fortnightly tide and two sites of observation, Iceland (blue curve) and Equator (green dashed line). The second component of volcanic seismic tremor corresponding to the fortnightly tide, is also shown for comparison (magenta).

tides are related to the Moon. Semi-diurnal and diurnal periods may exist in our data sets but their contribution is clearly absent (Fig. 3).

We identify 5-6 tidal periods common to both seismic tremor and VRP time-series as well as two tides detected only in the seismic tremor and one in the VRP (Fig. 3 and Table 1). The two time-series we considered correspond to the transfer of magma from the upper crust to its emission at Earth's surface with lava flows. These observations highlight that magma flow whatever its propagation media, e.g. Earth surface or upper crust, is modulated by lunisolar forces. The gradual decline characterizing the overall evolution of the eruption, identified through the trends by SSA (Fig. 3 and Supplementary, Figure S1) have been explained by interaction of pressure sources (magma body, its subsiding reservoir roof and subsurface flow path; Gudmundsson et al. (2016); Coppola et al. (2017)). Our study focuses on the smaller-magnitude variations and suggests that lunisolar forces interacted with these pressure sources hence contributing to maintain the flow of magma over the 6 months of eruption. This is evidenced by 1) the second-order variations that are very-well reconstructed using SSA and 2) by the fact that Earth tides amount to 50% of the two time-series.

The measurement techniques, ground and satellite based, the nature of the parameters measured, and the media where the magma propagated/flowed (Coppola et al. (2019)) may explain how differently tides contribute to each signal and therefore the differences observed between the two time-series over the 6 months. By extracting SSA components, we have not only been able to identify specific components composing our time-series but the waveforms. The two components associated with the strongest lunar tides identified in our data, e.g. the fortnightly and the monthly ones, start in phase with those of the l.o.d. (Fig. 4). Our calculations of the tidal potential (Fig. 5) confirmed this simultaneity, that is specific to the latitude of Iceland and the eruption timing. Moreover, the eruption initiated close to a minimum of the tidal potential (Fig. 5b) corresponding to a syzygy, a specific alignment of the Sun, Moon and Earth. Minima and maxima of the tidal potential are associated with the alignment of these celestial bodies in opposition or conjunction respectively. They have been both evoked to promote eruptive activity (Sottili and Palladino (2012) and references therein). The six-month eruption at Holuhraun initiated two days after a 4-hour eruption (Sigmundsson et al. (2015); Pedersen et al. (2017)). It was suggested that there was not a sufficient pressure at the dyke tip after its propagation over 48 km, to feed a long-lasting eruption (Woods et al. (2019)). No phase shift is observed between the strongest Earth tides and the seismic tremor from 29 to 31 August, and therefore we suggest that the Earth tides may have played a role in the triggering of the first small eruption on 29 August.

5. Conclusion

With this study, we focus on the 2014-2015 Holuhraun eruption (Iceland) and its temporal evolution as recorded by the seismic tremor and the power radiated by the lava field. We analyze the two geophysical time-series using Singular Spectrum Analysis (SSA) and we identify periods from ~5 to ~32 days. By applying a similar approach to the length-of-day (l.o.d.) measurements, considered as a relevant measure of the tidal actions on the Earth, we show that these different periods coincide with 6-8 periods of Earth tides. We estimate that ~50% of both signals are composed of tidal periods suggesting that magma movements follow frequencies imposed by lunisolar forces within the crust and at

Earth's surface. Moreover, by calculating the tidal potential for the Holuhraun eruption in Iceland, we suggest that Earth tides through their interaction with the pressure of the magma reservoir may have contributed to the triggering of the first (4-hour) eruption, on 29 August 2014.

Declaration of competing interest

The authors declare that they have no known competing financial interests or personal relationships that could have appeared to influence the work reported in this paper.

Acknowledgements

We thank the Editor Miaki Ishii for handling this manuscript and Gianluca Sottili and another anonymous reviewer for their thoughtful comments. SD would like to thank the Fundação para a Ciência e a Tecnologia (FCT) for his financial support through the postdoctoral grant (SFRH/BPD/17714/2016), as part of Human Capital Operating Programme (POCH) and the European Union. This work was supported by the Instituto Dom Luiz (IDL) through the FCT project UIDB/50019/2020 and partly supported by the H2020 project EUROVOLC, funded by the European Commission (Grant 731070). This is IPGP contribution number 4109.

Author contributions

S.D. led this research and the writing. S.D. performed the SSA analysis with F.L. J.L.L.M., F.L. and V.C. helped with the identification of tidal periods and the mechanism. F.S. contributed to the evaluation of the SSA analysis and the tidal effects on volcanoes. E.P.S.E. and C.J.B. analyzed the seismic data and D.C. the volcanic radiated power. All authors contributed to discuss the results and the writing of this manuscript.

Appendix A. Supplementary material

Supplementary material related to this article can be found online at https://doi.org/10.1016/j.epsl.2020.116145.

References

Ágústsdóttir, T., Woods, J., Greenfield, T., Green, R.G., White, R.S., Winder, T., Brandsdóttir, B., Steinthórsson, S., Soosalu, H., 2016. Strike-slip faulting during the 2014 Bárðarbunga-Holuhraun dike intrusion, central Iceland. Geophys. Res. Lett. 43, 1495–1503. https://doi.org/10.1002/2015GL067423.

Bredemeyer, S., Hansteen, T.H., 2014. Synchronous degassing patterns of the neighbouring volcanoes Llaima and Villarrica in South-central Chile: the influence of tidal forces. Int. J. Earth Sci. 103, 1999–2012. https://doi.org/10.1007/s00531-014-1037-2.

Cigolini, C., Poggi, P., Ripepe, M., Laiolo, M., Ciamberlini, C., Delle Donne, D., Ulivieri, G., Coppola, D., Lacanna, G., Marchetti, E., et al., 2009. Radon surveys and real-time monitoring at Stromboli volcano: influence of soil temperature, atmospheric pressure and tidal forces on 222Rn degassing. J. Volcanol. Geotherm. Res. 184, 381–388. https://doi.org/10.1016/j.jvolgeores.2009.04.019.

Coppola, D., Barsotti, S., Cigolini, C., Laiolo, M., Pfeffer, M., Ripepe, M., et al., 2019. Monitoring the time-averaged discharge rates, volumes and emplacement style of large lava flows by using MIROVA system: the case of the 2014-2015 eruption at Holuhraun (Iceland). Ann. Geophys. 61. https://doi.org/10.4401/ag-7749.

Coppola, D., Laiolo, M., Cigolini, C., Delle Donne, D., Ripepe, M., 2016. Enhanced volcanic hot-spot detection using MODIS ir data: results from the MIROVA system. Geol. Soc. (Lond.) Spec. Publ. 426, 181–205. https://doi.org/10.1144/SP426.5.

Coppola, D., Ripepe, M., Laiolo, M., Cigolini, C., 2017. Modelling satellite-derived magma discharge to explain caldera collapse. Geology 45, 523–526. https://doi.org/10.1130/G38866.1.

Custodio, S.I., Fonseca, J.F., d'Oreye, N.F., Faria, B.V., Bandomo, Z., 2003. Tidal modulation of seismic noise and volcanic tremor. Geophys. Res. Lett. 30. https://doi.org/10.1029/2003GL016991.

Dinger, F., Bobrowski, N., Warnach, S., Bredemeyer, S., Hidalgo, S., Arellano, S., Galle, B., Platt, U., Wagner, T., 2018. Periodicity in the BrO/SO_2 molar ratios in the volcanic gas plume of Cotopaxi and its correlation with the Earth tides during the eruption in 2015. Solid Earth 9, 247–266. https://doi.org/10.5194/se-2017-89.

Dumont, S., Sigmundsson, F., Parks, M.M., Drouin, V.J., Pedersen, G., Jónsdóttir, I., Höskuldsson, Á., Hooper, A., Spaans, K., Bagnardi, M., et al., 2018. Integration of sar data into monitoring of the 2014–2015 Holuhraun eruption, Iceland: contribution of the Icelandic volcanoes supersite and the FutureVolc projects. Front. Earth Sci. 6, 231. https://doi.org/10.3389/feart.2018.00231.

Dzurisin, D., 1980. Influence of fortnightly Earth tides at Kilauea volcano, Hawaii. Geophys. Res. Lett. 7, 925–928. https://doi.org/10.1029/GL007i011p00925.

Eibl, E.P., Bean, C.J., Jónsdóttir, I., Höskuldsson, A., Thordarson, T., Coppola, D., Witt, T., Walter, T.R., 2017a. Multiple coincident eruptive seismic tremor sources during the 2014–2015 eruption at Holuhraun, Iceland. J. Geophys. Res., Solid Earth 122, 2972–2987. https://doi.org/10.1002/2016JB013892.

Eibl, E.P., Bean, C.J., Vogfjörd, K.S., Ying, Y., Lokmer, I., Möllhoff, M., O'Brien, G.S., Pálsson, F., 2017b. Tremor-rich shallow dyke formation followed by silent magma flow at Bárðarbunga in Iceland. Nat. Geosci. 10, 299–304. https://doi.org/10.1038/ngeo2906.

Emter, D., 1997. Tidal triggering of earthquakes and volcanic events. In: Tidal Phenomena. Springer, pp. 293–309.

Girona, T., Huber, C., Caudron, C., 2018. Sensitivity to lunar cycles prior to the 2007 eruption of Ruapehu volcano. Sci. Rep. 8, 1476. https://doi.org/10.1038/s41598-018-19307.

Golub, G., Kahan, W., 1965. Calculating the singular values and pseudo-inverse of a matrix. J. Soc. Ind. Appl. Math., Ser. B Numer. Anal. 2, 205–224. https://doi.org/10.1137/0702016.

Gudmundsson, M.T., Högnadóttir, T., 2007. Volcanic systems and calderas in the Vatnajökull region, central Iceland: constraints on crustal structure from gravity data. J. Geodyn. 43, 153–169. https://doi.org/10.1016/j.jog.2006.09.015.

Gudmundsson, M.T., Jónsdóttir, K., Hooper, A., Holohan, E.P., Halldórsson, S.A., Ófeigsson, B.G., Cesca, S., Vogfjörd, K.S., Sigmundsson, F., Högnadóttir, T., et al., 2016. Gradual caldera collapse at Bárdarbunga volcano, Iceland, regulated by lateral magma outflow. Science 353, aaf8988. https://doi.org/10.1126/science.aaf8988.

Guinot, B., 1973. Variation du pôle et de la vitesse de rotation de la Terre. In: Traité de Géophysique Interne, Tome I: Sismologie et Pesanteur. MASSON & Cie, Éditeurs.

Hamilton, W.L., 1973. Tidal cycles of volcanic eruptions: fortnightly to 19 yearly periods. J. Geophys. Res. 78, 3363–3375. https://doi.org/10.1029/JB078i017p03363.

Jault, D., Le Mouël, J., 1991. Exchange of angular momentum between the core and the mantle. J. Geomagn. Geoelectr. 43, 111–129. https://doi.org/10.5636/jgg.43.111.

Jentzsch, G., Haase, O., Kroner, C., Winter, U., 2001. Mayon volcano, Philippines: some insights into stress balance. J. Volcanol. Geotherm. Res. 109, 205–217. https://doi.org/10.1016/S0377-0273(00)00312-7.

Jobert, G., Coulomb, J., 1973. Traité de Géophysique Interne, Tome I: Sismologie et Pesanteur. MASSON & Cie, Éditeurs.

Johannesson, H., Saemundsson, K., 2009. Geological Map of Iceland, Tectonics 1:600.000. Institute of Natural History, Gardabaer.

Kittler, J., Young, P.C., 1973. A new approach to feature selection based on the Karhunen-Loeve expansion. Pattern Recognit. 5, 335–352. https://doi.org/10.1016/0031-3203(73)90025-3.

Lambeck, K., 2005. The Earth's Variable Rotation: Geophysical Causes and Consequences. Cambridge University Press.

Lambert, S., Sottili, G., 2019. Is there an influence of the pole tide on volcanism? Insights from Mount Etna recent activity. Geophys. Res. Lett. 46, 13730–13736. https://doi.org/10.1029/2019GL085525.

Le Mouël, J., Lopes, F., Courtillot, V., Gibert, D., 2019. On forcings of length of day changes: from 9-day to 18.6-year oscillations. Phys. Earth Planet. Inter. 292, 1–11. https://doi.org/10.1016/j.pepi.2019.04.006.

Lopes, F., Le Mouël, J.L., Gibert, D., 2017. The mantle rotation pole position. a solar component. C. R. Géosci. 349, 159–164. https://doi.org/10.1016/j.crte.2017.06.001.

van Manen, S.M., Kervyn, M., Blake, S., Ernst, G.G., 2010. Apparent tidal influence on magmatic activity at Oldoinyo Lengai volcano, Tanzania, as observed in moderate resolution imaging spectroradiometer (MODIS) data. J. Volcanol. Geotherm. Res. 189, 151–157. https://doi.org/10.1016/j.jvolgeores.2009.11.003.

Martin, D.P., Rose Jr, W.I., 1981. Behavioral patterns of Fuego volcano, Guatemala. J. Volcanol. Geotherm. Res. 10, 67–81. https://doi.org/10.1016/0377-0273(81)90055-X.

Mauk, F., Johnston, M., 1973. On the triggering of volcanic eruptions by Earth tides. J. Geophys. Res. 78, 3356–3362. https://doi.org/10.1029/JB078i017p03356.

Mauk, F., Kienle, J., 1973. Microearthquakes at St. Augustine volcano, Alaska, triggered by Earth tides. Science 182, 386–389. https://doi.org/10.1126/science.182.4110.386.

McMillan, T.C., Rau, G.C., Timms, W.A., Andersen, M.S., 2019. Utilizing the impact of Earth and atmospheric tides on groundwater systems: a review reveals the future potential. Rev. Geophys. 57, 281–315. https://doi.org/10.1029/2018RG000630.

Melnik, O., Sparks, R.S.J., Costa, A., Barmin, A., et al., 2008. Volcanic eruptions: cyclicity during lava dome growth. In: Meyers: Encyclopedia of Complexity and Systems Science. Springer.

Neuberg, J., 2000. External modulation of volcanic activity. Geophys. J. Int. 142, 232–240. https://doi.org/10.1046/j.1365-246x.2000.00161.x.

Palladino, D.M., Sottili, G., 2014. Earth's spin and volcanic eruptions: evidence for mutual cause-and-effect interactions? Terra Nova 26, 78–84. https://doi.org/10.1111/ter.12073.

Parks, M.M., Heimisson, E.R., Sigmundsson, F., Hooper, A., Vogfjörd, K.S., Árnadóttir, T., Ófeigsson, B., Hreinsdóttir, S., Hjartardóttir, Á.R., Einarsson, P., et al., 2017. Evolution of deformation and stress changes during the caldera collapse and dyking at Bárdarbunga, 2014–2015: implication for triggering of seismicity at nearby Tungnafellsjökull volcano. Earth Planet. Sci. Lett. 462, 212–223. https://doi.org/10.1016/j.epsl.2017.01.020.

Patanè, G., Frasca, A., Agodi, A., Imposa, S., 1994. Earth tides and Etnean volcanic eruptions: an attempt at correlation of the two phenomena during the 1983, 1985 and 1986 eruptions. Phys. Earth Planet. Inter. 87, 123–135. https://doi.org/10.1016/0031-9201(94)90026-4.

Pedersen, G., Höskuldsson, A., Dürig, T., Thordarson, T., Jonsdottir, I., Riishuus, M.S., Óskarsson, B., Dumont, S., Magnússon, E., Gudmundsson, M.T., et al., 2017. Lava field evolution and emplacement dynamics of the 2014–2015 basaltic fissure eruption at Holuhraun, Iceland. J. Volcanol. Geotherm. Res. 340, 155–169. https://doi.org/10.1016/j.jvolgeores.2017.02.027.

Petrosino, S., Cusano, P., Madonia, P., 2018. Tidal and hydrological periodicities of seismicity reveal new risk scenarios at Campi Flegrei caldera. Sci. Rep. 8, 1–12. https://doi.org/10.1038/s41598-018-31760-4.

Pfeffer, M.A., Bergsson, B., Barsotti, S., Stefánsdóttir, G., Galle, B., Arellano, S., Conde, V., Donovan, A., Ilyinskaya, E., Burton, M., et al., 2018. Ground-based measurements of the 2014–2015 Holuhraun volcanic cloud (Iceland). Geosciences 8, 29. https://doi.org/10.3390/geosciences8010029.

Ray, R.D., Erofeeva, S.Y., 2014. Long-period tidal variations in the length of day. J. Geophys. Res., Solid Earth 119, 1498–1509. https://doi.org/10.1002/2013JB010830.

Ricco, C., Petrosino, S., Aquino, I., Del Gaudio, C., Falanga, M., 2019. Some investigations on a possible relationship between ground deformation and seismic activity at Campi Flegrei and Ischia volcanic areas (southern Italy). Geosciences 9, 222. https://doi.org/10.3390/geosciences9050222.

Schultz, R.A., 1996. Relative scale and the strength and deformability of rock masses. J. Struct. Geol. 18, 1139–1149. https://doi.org/10.1016/0191-8141(96)00045-4.

Sigmundsson, F., Hooper, A., Hreinsdóttir, S., Vogfjörd, K.S., Ófeigsson, B.G., Heimisson, E.R., Dumont, S., Parks, M., Spaans, K., Gudmundsson, G.B., et al., 2015. Segmented lateral dyke growth in a rifting event at Bárðarbunga volcanic system, Iceland. Nature 517, 191–195. https://doi.org/10.1038/nature14111.

Sottili, G., Martino, S., Palladino, D., Paciello, A., Bozzano, F., 2007. Effects of tidal stresses on volcanic activity at Mount Etna, Italy. Geophys. Res. Lett. 34. https://doi.org/10.1029/2006GL028190.

Sottili, G., Palladino, D.M., 2012. Tidal modulation of eruptive activity at open-vent volcanoes: evidence from Stromboli, Italy. Terra Nova 24, 233–237. https://doi.org/10.1111/j.1365-3121.2012.01059.x.

Sottili, G., Palladino, D.M., Cuffaro, M., Doglioni, C., 2015. Earth's rotation variability triggers explosive eruptions in subduction zones. Earth Planets Space 67, 208. https://doi.org/10.1186/s40623-015-0375-z.

Sparks, R., 1981. Triggering of volcanic eruptions by Earth tides. Nature 290, 448. https://doi.org/10.1038/290448a0.

Stothers, R.B., 1989. Volcanic eruptions and solar activity. J. Geophys. Res., Solid Earth 94, 17371–17381. https://doi.org/10.1029/JB094iB12p17371.

Vautard, R., Ghil, M., 1989. Singular spectrum analysis in nonlinear dynamics, with applications to paleoclimatic time series. Phys. D, Nonlinear Phenom. 35, 395–424.

Vautard, R., Yiou, P., Ghil, M., 1992. Singular-spectrum analysis: a toolkit for short, noisy chaotic signals. Phys. D, Nonlinear Phenom. 58, 95–126.

Williams-Jones, G., Stix, J., Heiligmann, M., Barquero, J., Fernandez, E., Gonzalez, E., 2001. A model of degassing and seismicity at Arenal volcano, Costa Rica. J. Volcanol. Geotherm. Res. 108, 121–139. https://doi.org/10.1016/S0377-0273(00)00281-X.

Woods, J., Winder, T., White, R.S., Brandsdóttir, B., 2019. Evolution of a lateral dike intrusion revealed by relatively-relocated dike-induced earthquakes: the 2014–15 Bárðarbunga–Holuhraun rifting event, Iceland. Earth Planet. Sci. Lett. 506, 53–63. https://doi.org/10.1016/j.epsl.2018.10.032.